Organic fertilizer as a chelating agent in photo-Fenton at neutral pH with LEDs for agricultural wastewater reuse: micropollutant abatement and bacterial inactivation

N. López-Vinent[a], A. Cruz-Alcalde[a], J. A. Malvestiti[b], P. Marco[a], J. Giménez[a]*, S. Esplugas[a]

aDepartment of Chemical Engineering and Analytical Chemistry, Faculty of Chemistry, Universitat de Barcelona, C/Martí i Franqués 1, 08028 - Barcelona, Spain. Tel: +34934021293. Fax: +34934021291

bSchool of Technology, University of Campinas –UNICAMP, Paschoal Marmo 1888, 13484332, Limeira-SP, Brazil

Corresponding Author: j.gimenez.fa@ub.edu

ABSTRACT

In a water scarcity scenario, the reused wastewater could be an essential source for agricultural irrigation considering that 60% of fresh water is destined to this area. In this study, an organic fertilizer (Diethylene triamine pentaacetic acid, DTPA) was used as a new chelating agent of iron for photo-Fenton's application at neutral pH using LEDs. Secondary effluents with different characteristics were tested for propranolol removal and bacterial inactivation. With DTPA, the best results were achieved with MBR matrix: 94.0% of propranolol removal and total bacterial inactivation after 120 min. IFAS matrix showed the worst results: 63.2% of propranolol removal and only 2-log reduction for Total Coliforms. The performance of DTPA as chelating agent was compared with EDTA and EDDS with two matrices. In MBR matrix, propranolol removal with EDTA was 100% in 15 minutes, while DTPA and EDDS reached similar results at 120 minutes (94.0

and 91.3%), respectively. The iron precipitation was evaluated, and DTPA showed high stability with Fe^{2+} (only 10.4% of iron reduction instead 97.3% for EDDS). In addition, it looks like that the stability of iron chelates plays an important role in bacterial inactivation. Thus, the experiments with DTPA showed the lowest bacterial growth-on-the-plate after 72 hours of the end of the experiment. Biodegradability and phytotoxicity were also evaluated and the experiments with DTPA had the lowest toxicity. The results of the experiments performed with DTPA were compared with the values in *Proposal for agricultural water reuse* suggesting that treated effluent accomplish the requirements for agriculture.

KEYWORDS

1. Introduction

The World Wildlife Fund (WWF) estimates that two-thirds of the world's population may face water shortage by 2025 at the current water consumption rate. Many of the water systems, which maintain ecosystems flourishing and provide water for human population, have changed into stressed [1]. All of that have forced to scientific community to investigate more efficient technologies for wastewater (WW) treatment and reuse [2]. Reused WW could be an important source of irrigation in the scarcity water scenario. According to UNESCO (The United Nations Educational, Scientific and Cultural Organization), the water consumed by agriculture is between 60 and 70% of fresh water, and this amount can increase up to 89% by 2025. Nevertheless, the quality of the reused WW must ensure the maintenance of an adequate level of public health and environmental protection. The key parameters can be found in the Proposal for a Regulation of the European Parliament and of the Council on minimum requirements for water reuse. This

proposal establishes key parameters concerning pathogens [3]. However, in view of future WW reuse laws, micropollutants (MPs) probably will be regulated. So far, in the field of water policy, two regulations have been released in order to identify priority substances in water: Directive 2013/39/UE, which establish a list of priority compounds and environmental quality standards for these substances and other compounds [4], and Decision (EU) 2018/840, establishing a watch list of substances for monitoring in the field of water policy [5].

In the last decades, Advanced Oxidation Processes (AOPs) have proven to be efficient in the removal of large amount of non-biodegradable and recalcitrant compounds [6-9], which are not removed in conventional Wastewater Treatment Plants (WWTPs) [10-13]. In addition, there are some disadvantages related to conventional methods used for disinfection of WW, for instance chlorination [14]. The generation of disinfection by-products (DBPs), like trihalomethanes, is risky to human health and aquatic ecosystems [15]. Among AOPs, the photo-Fenton process is one of the most effective for disinfection and MPs abatement [16-18]. However, the optimal conditions of this process (acid pH) can make it unattractive for its application at full scale [19, 20]. In this way, several chelating agents have been tested in order to operate at neutral pH. Citrate, oxalate, EDTA (Ethylenedinitrilotetraacetic acid) and EDDS (Ethylenediamine-N, N'-disuccinic acid) are the most common chelating agents used in photo-Fenton process [21]. However, there are no data, as far as we have been able to investigate, in the assessment of DTPA (Diethylene triamine pentaacetic acid) as chelating agent in photo-Fenton process. This compound is used in different processes, mainly in agriculture and horticulture as an organic fertilizer. For instance, DTPA is included in the register of fertilizer products of the Ministry of Agriculture, Fisheries and Food of the Spanish Government [22]. Thereby, if DTPA was used as chelating agent, the treated WW could be employed in

agriculture without needing to separate. The costs associated to electrical consumption by lamps are other disadvantage for the large-scale application of photo-Fenton process. These costs can be reduced when light emitting diodes (LEDs) are used in comparison with conventional lamps. No mercury content, low power consumption, long lifetime and no overheating are the main advantages in the replacement of conventional lamps by LEDs.

Therefore, the focus of this work is to test the efficiency of DTPA as a chelating agent in photo-Fenton at neutral pH using LEDs. Four different WW of secondary effluents from two WWTPs (located in Barcelona, Spain) were used with different characteristics. In addition, EDTA and EDDS (two of the most used chelating agents) were compared with DTPA in the MPs removal. In this case, propranolol (PROP) was selected as a target compound. This compound is a type of non-selective drug called beta-blocker and it is the one with the greatest presence in the aquatic environments [23]. Their occurrence in rivers or wastewaters was detected in concentrations ranging from 0.1-7.3 ng·L^{-1} [24, 25]. In surface waters was found in concentration of 53 ng·L^{-1} [26]. In addition, their presence was found in different countries: Spain, Croatia, France, Serbian, Bosnian and China [24, 27-30]. Bacterial disinfection (*E. coli* and Total coliforms) was also evaluated. The changes of biodegradability and toxicity (*Vibrio Fishery* and phytotoxicity) of the treated effluents are also important to know if the treated water satisfy the requirements for agricultural use [3].
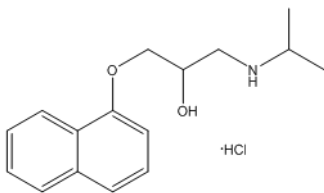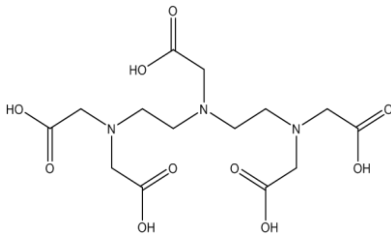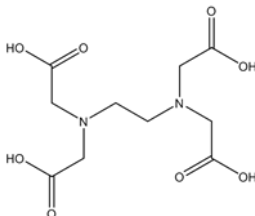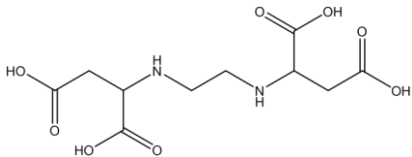
2. Material and methods

2.1. Chemicals

Propranolol hydrochloride, EDDS-Na solution, DTPA (99%), hydrogen peroxide (H$_2$O$_2$) (30% *w/v*), Chromocult® Coliform Agar and catalase from bovine liver were obtained

from Sigma-Aldrich. Ferrous sulfate ($FeSO_4 \cdot 7H_2O$), EDTA, acetonitrile and orthophosphoric acid were purchased from Panreac Quimica. Buffered peptone water was acquired from Labkem. The following table (Table 1) shows the properties of target compound and different chelating agents used in this work.

Table 1. Properties of propranolol and three chelating agents tested in this study.

Compound	Molecular formula	Chemical structure	Molecular weight (g/mol)
PROP	$C_{16}H_{12}NO_2 \cdot HCl$		295.81
DTPA	$C_{14}H_{23}N_3O_{10}$		393.35
EDTA	$C_{10}H_{16}N_2O_8$		292.24
EDDS	$C_{10}H_{16}N_2O_8$		292.24

2.2. Real WW effluents

The experiments were performed with four different WW. The effluents were acquired from the Gavà and El Prat de Llobregat WWTPs (province of Barcelona, Spain) after the biological treatment. Table 2 shows the main parameters of these WW.

Each WWTP presents two secondary treatments in parallel. WWTP of Gavà has Membrane Bioreactor (MBR) and Integrated Fixed-Film Activated Sludge (IFAS). WWTP of El Prat de Llobregat includes Conventional Activated Sludge (CAS) and the same treatment with nutrients elimination (CAS-NE) where the removal of 70% of phosphorus and nitrogen takes place.

Table 2. Parameters of the tested effluents before spike target compound. N/A: below the detection level.

Parameters	IFAS	MBR	CAS	CAS-NE
pH	7.9	7.8	8.0	7.6
Turbidity (NTU)	13.9	1.0	8.9	4.0
UV_{254} (m^{-1})	48	0.3	29	13
TOC (mg C $\cdot$ L^{-1})	29.5	5.3	24.1	7.9
DOC (mg C $\cdot$ L^{-1})	22.2	4.7	20.9	5.1
Total alkalinity (mg $CaCO_3 \cdot L^{-1}$)	545	312	457	304
Cl^{-1} (mg$\cdot L^{-1}$)	507	470	519	482
SO_4^{2-} (mg$\cdot L^{-1}$)	152	125	242	236
$N\text{-}NO_2^-$ (mg$\cdot L^{-1}$)	N/A	N/A	N/A	N/A
$N\text{-}NO_3^-$ (mg$\cdot L^{-1}$)	N/A	9.9	24.8	31.7

2.3. Experimental procedure

All experiments were performed with real WW and carried out in a UV-A LED tubular photoreactor composed with 8 LEDs (wavelength 365 nm; irradiance: $2.66 \cdot 10^{-7}$ Einstein$\cdot$L$^{-1} \cdot$ s^{-1}). More information about the installation can be found in a supplementary material in figure S1. Each LED has 1.05 W of nominal power and 125º of irradiance angle. The 1 L of solution to be treated arrived to photoreactor from a feeding tank and it was continuously recirculated to the tank, where it was magnetically stirred. The temperature was maintained constant at 25º (Haake C-40) during all the experiment.

Real WW was taken out of the fridge a few hours before the experiment started for bacterial acclimation. To prepare the solutions, the respective chelating agent (EDDS, EDTA or DTPA) in each experiment was added to real WW. When this was dissolved, Fe(II) (0.18 mM) was put into the solution to form the complex. The molar ratios chelating agent:Fe(II) were 1:1 for EDTA and DTPA and 2:1 for EDDS, based on previous experiments. Finally, PROP (1.9 µM) was spiked to the solution. This concentration was selected to perform the study more realistic comparing with the PROP concentrations detected in the aquatic ecosystems. At the same time, this concentration allows a good monitoring of PROP. Hydrogen peroxide (4.41 mM) was added just before to start the experiment. Samples were withdrawn from the photoreactor at different times for 120 minutes. To stop the Fenton reaction, 10 µL of bovine catalase solution (200 mg$\cdot$L^{-1}) was added to 5 mL of each sample to decompose H_2O_2.

2.4. Analytical measurements

Hydrogen peroxide concentration was determined by colorimetric method based on the use of metavanadate [31] which forms a stable yellow complex with H_2O_2 and absorbs at 410 nm. Total iron in solution was measured at 510 nm by the o-phenatroline procedure (ISO 6332). The concentration of target compound at each time was monitored by HPLC

Infinity Series (Agilent) and C-18 column (Tecknokroma) (250 x 4.6 mm i.d; 5µm particle size). According to the absorbance of PROP the UV detector worked at 214 nm. Acetonitrile and orthophosphoric water solution (pH=3) were used as a mobile phase (25:75, respectively). An injection volume of 100 µL and 0.7 mL·min^{-1} of flux were fixed. Biochemical Oxygen Demand (BOD) was performed following the 5210-standard method. Phytotoxicity was determined according Tam and Tiquia [32] using *Lactuca sativa* (lettuce) seeds. More information can be found in Table S1 in supplementary information. Acute toxicity was performed with Microtox M500 (*Vibrio Fishery*). Bacterial inactivation analyses were performed with 1 mL of each sample, where catalase was added to remove residual H_2O_2. This volume was plated on Chromocult® Coliform Agar before prepared in the laboratory. When a dilution was needed, buffered peptone water was used. Standard plated counted method was employed after an incubation period of 24 h at 35º. Growth-on-the-plate was determined for 48 and 72 hours in the same plates of 120 minutes incubated at 35º.

3. Results and discussion

3.1. Effect of DTPA on photo-Fenton process

The efficiency of organic fertilizer (DTPA) as chelating agent was studied in the PROP abatement by neutral photo-Fenton with UV-A LEDs (Figure 1). Due to the novelty in the use of DTPA as chelating agent in photo-Fenton process, some preliminary tests were performed to determine the optimum molar ratio Ligand:Fe(II) (Supplementary material Figure S2 and Table S2). At the beginning of the experiment, total iron was chelated using 1:1 L:Fe(II) molar ratio and PROP degradation was faster. Thus, this L:Fe(II) molar ratio was employed in the rest of experiments with DTPA. Evaluation was performed in four wastewaters, which characteristics differ considerably (see Table 2), implying different

behaviors in the MP removal. The photo-Fenton experiments were carried out at the natural pH of the effluents (between 7.6 and 8.0, according to table 2).
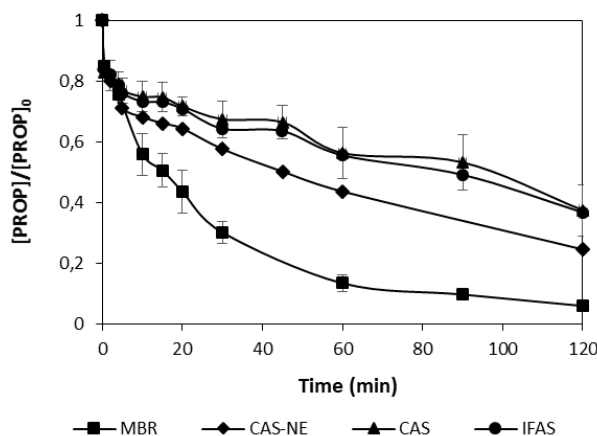
Figure 1. Propranolol removal by UV-A LEDs circumneutral photo-Fenton process catalyzed by DTPA:Fe(II) in four different WWs. $[PROP]_0 = 1.9$ μM; $[Fe(II)]_0 = 0.18$ mM; $[H_2O_2] = 4.41$ mM; L:Fe(II) molar ratio = 1:1.

Among different WWs, MBR showed higher degradation compared to other three wastewaters, achieving 94.0% PROP removal after 120 minutes (0.63 kJ·L^{-1}). However, only 63.2% and 62.5% were removed in 120 min for IFAS and CAS, respectively, being the worst. PROP abatement in CAS-NE was 75.4% at the end of the experiment. As known, real wastewaters are complicated matrix because of the different compounds present. As it can observed in table 2, MBR presents low TOC (Total Organic Carbon) and turbidity. Nevertheless, the same parameters in IFAS were the highest. The PROP removal is related to TOC values and decreases when TOC increases. The kinetic constants of the reaction between hydroxyl radical and DOM depend largely on the type of organic matter present in the matrix. However, some authors have quantified the kinetic constants between 10^8-10^9 L·molC^{-1}·s^{-1} [33-38]. In this way, less organic matter produces less competition for hydroxyl radicals. The turbidity is also important in terms of the light scattering. CAS-NE presents approximately 2 times and 3 times lower turbidity than CAS and IFAS, respectively. In MBR the turbidity was approximately 9 times lower than in CAS and 14 times lower than in IFAS.

In order to better explain the results of MP abatement in different wastewaters two different fittings to a first order kinetics (Table 3) were performed for the different WW effluents. The kinetic constant k_1 represents the fitting in the first 30 seconds and it is strongly related to the initial reaction rate. While k_2 is the fitting from 30 seconds until 120 minutes. A first order kinetics was assumed according to eq.1.

$$\ln \left(\frac{c_f}{c_0} \right) = k \cdot t \qquad \qquad \textbf{(Eq.1)}$$

Table 3. Kinetic constants obtained for photo-Fenton catalyzed by DTPA:Fe(II) in different wastewaters at initial time (0-30 s) and between 30 s and 120 min (fitting to a first order kinetics). Values of R^2 of k_1 are not shown due to only two points were used..

Wastewaters	k_1 (min^{-1})	k_2 (min^{-1})	R^2 k_2
MBR	0.324	0.022	0.97
CAS-NE	0.350	0.009	0.99
CAS	0.375	0.006	0.96
IFAS	0.321	0.004	0.97

As it can observed in table 3, the values of k_1 were practically the same in the four WWs even presenting different values of TOC and turbidity. In addition, k_1 was higher than k_2 in all WWs. This fact evidences that the dark Fenton process controls the reaction rate in first 30 seconds, as explained in previous works [17]. The differences due to the matrix were appreciated when k_2 was calculated. The values of k_2 decrease when TOC and turbidity increase (see Table 2). Thus, MBR presents the highest rate and IFAS the lowest. These facts seem to indicate that photo-Fenton controls the reaction rate after the first 30 seconds. This means that light plays an important role which can explain that k_2 decreases

when turbidity and TOC increase, because light scattering or light absorption can increase. Thus, as it can be seen in table 2, the turbidity of MBR is by the far the lowest and these differences were highlighted in the values of k_2.

3.2. Comparison with conventional chelating agents

Several authors have been proved the efficiency of different chelating agents in the photo-Fenton process at circumneutral pH: nitrilotriacetic acid (NTA) [39-41], oxalic acid (OA) [42-44], citric acid (Cit) [45-47], ethylenedinitrilotetraacetic acid (EDTA) [39, 48, 49], ethylenediamine-N,N'-disuccinic acid (EDDS) [20, 21, 37, 50-52] and DL-tartaric acid (TA) [39]. A problem related to the use of chelating agents is linked to the fact that the hydroxyl radicals generated in the Fenton's reaction also attack the complex of iron and chelating agent leaving iron in solution at neutral pH [39], producing the catalytic activity decrease due to the subsequent iron precipitation and chelating degradation. DTPA can help to address this problem. Thus, the next step is to compare the DTPA behavior with two of the most used chelating agents, such as EDTA and EDDS. The target compound was also PROP, in two WWs: CAS and MBR, dirty and clean WW, respectively. The L:Fe(II) molar ratios used were 1:1 for EDTA and DTPA and 2:1 for EDDS. These values were necessary to ensure the complete iron chelation at the beginning of the experiment. Figure 2 and 3 show the obtained results.
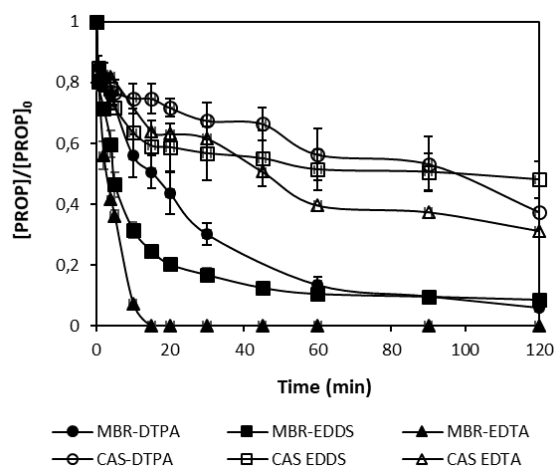
Figure 2. Propranolol removal by UV-A LEDs circumneutral photo-Fenton in CAS (open symbols) and MBR (closed symbols). $[PROP]_0 = 1.9$ μM; $[Fe(II)]_0 = 0.18$ mM; $[H_2O_2] = 4.41$ mM; EDTA:Fe(II) = 1:1; DTPA:Fe(II) = 1:1; EDDS:Fe(II) = 2:1.

As obvious, when MBR was tested, the three chelating agents presented better results than CAS, due to the highest TOC and turbidity of CAS, as explained above (section 3.1). Regarding the efficiency on PROP removal, the percentages reached in MBR at the end of the experiment (120 minutes, 0.63 kJ·L^{-1}) were 100%, 94.0% and 91.3% for EDTA, DTPA and EDDS, respectively. In CAS the removals were 68.7%, 62.5% and 51.9% in the same order.

In MBR matrix, EDTA presented the total PROP removal at 15 minutes of treatment (0.08 kJ·L^{-1}). However, for DTPA and EDDS at the same time (15min), the removal percentages were: 49.4% and 75.4%, respectively. EDDS presents a good removal at this time but then slows down a lot, achieving only 15.9% of degradation between 15 and 120 minutes. The explanation of this behavior can be related to iron precipitation. Iron content was monitored during each experiment, as represented in figure 3. In the course of the reaction, hydroxyl radicals attack PROP and the iron complex. This fact implies the

breaking of the complexes and subsequent iron precipitation, due to the neutral pH, provoking a decrease in the catalytic activity, as commented before.
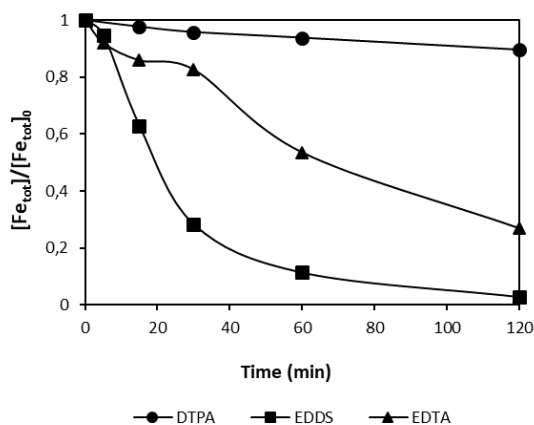
Figure 3. Trend of total dissolved iron during the reaction for EDTA, DTPA and EDDS in MBR matrix. $[PROP]_0 = 1.9$ μM; $[Fe(II)]_0 = 0.18$ mM; $[H_2O_2] = 4.41$ mM; EDTA:Fe(II) = 1:1; DTPA:Fe(II) = 1:1; EDDS:Fe(II) = 2:1.

As observed in figure 3, complex destruction started at 5 min of reaction for EDDS. After this, a gradual reduction of total dissolved iron was observed, with a reduction of 97.3% at the end of the experiment (120 min). Nevertheless, at 15 min of the experiment, 37.3% had already been decreased. This fact is in agreement with the high percentage of PROP removal achieved in 15 min with EDDS in MBR (see Figure 2). After this, the degradation slowed down a lot (see also Fig. 2), due to the precipitation of iron (see Fig. 3), which reduces the catalytic activity. For EDTA, a great amount of total dissolved iron was precipitated at the end of the experiment (72.9% of iron reduction). However, in this case, the precipitated iron at 15 min was only 14.1% (Fig. 3), which is in agreement with the fact that PROP was totally removed at 15 min (see Fig. 2), and this minimum reduction of total dissolved iron did not seem to be so important in the decrease of catalytic activity. Concerning DTPA, it is important to consider that only 10.4% of total dissolved iron precipitated after 120 minutes of the reaction. This fact shows the higher stability of the

chelate and its resistance against hydroxyl radicals and radiation when DTPA is used. The stability constants (k_{stab}) of each chelating agent and iron are specific for the iron species (k_{stab} DTPA-Fe(III) = 28.60, k_{stab} EDTA-Fe(III) = 25.10, k_{stab} EDDS-Fe(III) = 22.0, k_{stab} DTPA-Fe(II) = 16.55, k_{stab} EDTA-Fe(II) = 14.33) [53]. Data were not found about k_{stab} for EDDs-Fe(II). Nevertheless, always DTPA presents a high stability constant with iron. Thus, in DTPA the degradation was slower than with EDTA and EDDS, due to the high stability in chelation of iron, but a gradual PROP reduction was observed achieving even a higher PROP removal than EDDS at the end of the experiment (see Fig. 2). The stability of the metal chelates appears to be influenced by their chemical structure, mainly the number and strength of the Fe-ligand interactions. According to this, the additional amino group in the chemical structure of DTPA provides its complex with iron with a coordination number of 7 instead of 6, as is the case of EDTA and EDDS. Therefore, this results in a higher stability of the DTPA complex. The observed differences in the stability of EDTA and EDDS complexes are caused by the larger distance from the amino groups to the carboxylic extremes of the EDDS molecule compared to EDTA. This causes a weaker interaction between these groups and iron, leading thus to a lower overall stability of the resulting complex.

Concerning CAS, the differences between three chelating agents were not so significant than in MBR. In this case, the effect of iron precipitation was more pronounced for EDTA. As it can be observed in figure 3, in first 45 min (0.32 kJ·L^{-1}) of the experiment the degradation curves for EDTA and EDDS were very similar and removals obtained were 44.9% and 49.3% for EDDS and EDTA, respectively. When EDDS was used (between 15 and 120 min of the treatment) the degradation was very low due to the iron precipitation, as observed with MBR matrix. However, in EDTA system the iron precipitation was lower and approximately 70% of iron remains in solution at 45 min.

After that time, the PROP removal continued to increase in EDTA system until 60 min ($0.47 \ kJ \cdot L^{-1}$). Values of 48.6% and 60.4% of PROP removal were achieved at 60 min for EDDS and EDTA, respectively, proving that the iron precipitation is so important for the catalytic activity. However, at 60 minutes the iron leaching gradually increased in EDTA until the end of the experiment, decreasing the PROP removal (between these times of the reaction, the degradation curve significantly slowed down). When the organic fertilizer (DTPA) was used, the PROP degradation came down more slowly than EDTA and EDDS during the experiment. However, at the end of the treatment, the PROP removals achieved for different chelating agents were: 68.7%, 62.5% and 51.9% for EDTA, DTPA and EDDS, respectively. The high biodegradability of EDDS and low stability constant with iron caused the iron precipitation, generating low catalytic activity. Moreover, in EDDS the molar ratio L:Fe(II) was 2:1, but for EDTA and DTPA this ratio was 1:1. This increase in TOC, due to the presence of more EDDS, can also decrease the catalytic activity. For EDTA, degradation in CAS was slower than in MBR, because CAS has high TOC than MBR and, therefore, more influence of iron leaching was observed. Nevertheless, the high stability of DTPA with iron was essential to achieve close degradation than EDTA.

Summarizing, as it can be observed in Fig. 2, the reaction rate is very high at the beginning of the process (first 30 s) and similar for the two WW and the three chelating agents tested. This fact was due to the dark Fenton controls the reaction at first 30 seconds. Details of this behavior can be found in previous works [17, 54].

After this initial period, the reaction rate is strongly determined by the iron precipitation and therefore for the complex stability. DTPA forms a more stable chelate with iron, as seen in Fig. 3. This explains a slower profile in the reaction rate, as shown in Fig. 2. However, EDTA and EDDS form less stable chelates, especially EDDS (see Fig. 3).

Hence, between 30 s and 15 min, the break of the chelate allows more iron to be dissolved in the solution for a time and this would explain that the reaction rate is higher for EDTA and EDDS than for DTPA. However, in the last part of the experiment, between 15 and 120 min and according to Fig. 3, for EDDS practically no iron remains in solution and this implies that the reaction rate is drastically reduced. Thus, the iron in solution (Fig. 3), or the stability of the chelate, strongly determine the degradation rate of PROP (Fig. 2). Table S3 in the supplementary material shows a pseudo-quantitative explanation of all that. This commented behavior was observed for the two matrices tested (MBR and CAS) but reaction rates are little lower in CAS due to its high TOC and turbidity.

From this perspective, to rise the stability of iron chelates is advantageous to perform photo-Fenton at neutral pH, but the efficiency is also important [55]. It could be added that with EDTA and EDDS, due to iron precipitation, some mud is formed, which also interferes with the action of light and could help to explain, for example, the decrease of reaction rate for the EDDS.

3.3. Disinfection tests.

Along with micropollutants, an efficient wastewater disinfection processes is important to improve public health, mainly when the reuse is aimed [56]. Therefore, it is important to find a process capable to eliminate both pathogens and MPs. The quantification of total coliforms (TC) in the four WWs revealed the presence of 1.7×10^2, 1.8×10^2, 3.8×10^2 and 9.8×10^3 colony-forming units per 1 mL (CFU·mL^{-1}) at initial time for MBR, CAS-NE, CAS and IFAS, respectively. Initial concentrations of *E.coli* were 3×10^1 and 9×10^2 (CFU·mL^{-1}) for CAS and IFAS, respectively. In MBR and CAS-NE *E.coli* was not found. Figure 2A shows the TC inactivation and figure 2B the *E.coli* inactivation with photo-Fenton process catalyzed by DTPA:Fe(II). According to Ortega-Gómez *et al*, the

recirculation system (pump and flow) had no effect on cell viability [1]. Blank tests with only iron or hydrogen peroxide were performed and no inactivation was achieved with these concentrations.
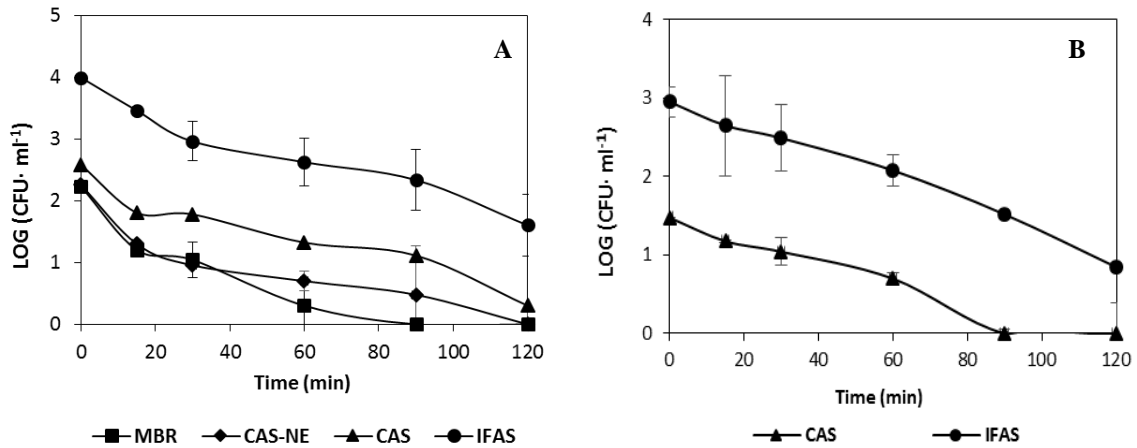

Figure 4. TC inactivation in four WWs (A) and *E.coli* inactivation in IFAS and CAS (B) with photo-Fenton process catalyzed by DTPA:Fe(II). $[PROP]_0 = 1.9$ μM; $[Fe(II)]_0 = 0.18$ mM; $[H_2O_2] = 4.41$ mM; L:Fe(II) molar ratio = 1:1.

According to Figure 4, the circumneutral photo-Fenton using DTPA as a chelating agent was effective for the disinfection of total coliforms in different water matrices. MBR and CAS-NE reached the total coliform disinfection at the end of the treatment. Concerning CAS and IFAS, total coliforms decreased 2 order of magnitude at 120 minutes. As it can be seen in Fig. 4A, the inactivation curves for MBR and CAS-NE were overlapped in the first 30 minutes. In addition, MBR, which is the cleanest matrix, presented a high reduction, arriving at 1 $CFU \cdot mL^{-1}$ at 90 minutes (0.47 $kJ \cdot L^{-1}$). However, in CAS-NE fewer reductions were observed in the next minutes (presenting 3 $CFU \cdot mL^{-1}$ at 90 min). CAS and IFAS presented the worst results in terms of $CFU \cdot mL^{-1}$. To compare with the other matrices, at 90 minutes values of 1.3 $x10^1$ and 2.16 x 10^2 $CFU \cdot mL^{-1}$ were obtained for CAS and IFAS, respectively. Obviously, IFAS is the one with the highest decrease in TC in absolute value, which is logical since it also has the highest initial value in TC.

However, when representing log TC versus time, as shown in Fig. 4A, the disappearance rate is lower in IFAS. It was tried to make different kinetic fittings to be able to compare the data mathematically but none of them offered good correlations. This is also logical considering that TC are living beings whose behavior has nothing to do with that of inert chemical compounds. However, it is observed that, at the beginning, the disappearance rate is much higher in MBR and CAS-NE than in IFAS. This could be related to the fact that the higher TOC and turbidity of IFAS also represents a greater competition for hydroxyl radicals, reducing efficiency in the elimination of TC in IFAS.

Initial concentrations of *E.coli* were 3×10^1 and 9×10^2 CFU·mL^{-1} for CAS and IFAS, respectively. *E.coli* inactivation (Figure 2B) followed similar trend than TC. At 90 min, 0 CFU·mL^{-1} was reached in CAS. However, in IFAS 2 orders of magnitude of inactivation were achieved at the end of the treatment. Nevertheless, 7 CFU·mL^{-1} were counted at 120 minutes. Again, the influence of the water matrix was present, leading to a significant difference in the inactivation time.

The disinfection activity of DTPA was also compared with EDTA and EDDs. In this case, CAS and MBR were selected for the chelating agents comparison (TC: 1.7×10^2 and 3.8×10^2 CFU·mL^{-1} at initial time for MBR and CAS, respectively; *E.Coli*: 3×10^1 CFU·mL^{-1} for CAS). Figure 5 shows the bacterial inactivation for different chelating agents in CAS and MBR.
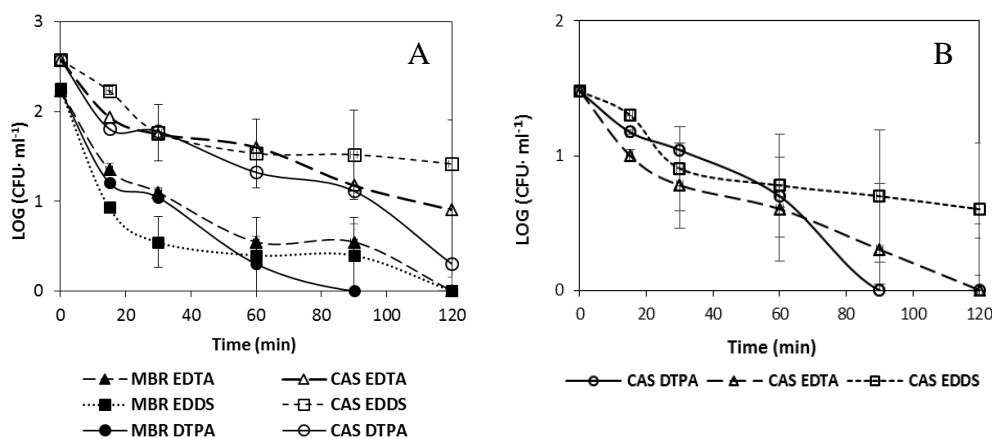
Figure 5. (A) TC inactivation in CAS and MBR for EDTA, EDDS and DTPA and (B) *E.coli* inactivation in CAS for EDTA, EDDS and DTPA with photo-Fenton process at circumneutral pH. $[PROP]_0 = 1.9$ µM; $[Fe(II)]_0 = 0.18$ mM; $[H_2O_2] = 4.41$ mM; EDTA:Fe(II) = 1:1; DTPA:Fe(II) = 1:1; EDDS:Fe(II) = 2:1.

As it can be seen, the photo-Fenton treatment reduced the bacterial concentration in TC (Fig. 5A) and *E.Coli* (Fig. 5B). MBR matrix achieved the best results arriving until 0 CFU·mL^{-1} at the end of the treatment for the three chelating agents. During the first 30 minutes of the treatment, EDDS showed higher reduction than EDTA and DTPA, followed by a slight reduction of TC the next 60 minutes (until 90 minutes of the experiment). DTPA and EDTA presented similar inactivation curves during the first 45 minutes. After this, DTPA showed a high inactivation rate, achieving the total TC inactivation at 90 minutes. After 60 min of the experiment the inactivation curves for EDTA and EDDS were very similar. The iron precipitation plays again an important role in hydroxyl radical formation, achieving DTPA good results due to the stability of the chelate (see Fig. 3). When CAS is used as water matrix, things change because the inactivation efficiency is deeply dependent on the characteristics of the matrix. At 120 minutes of the experiment, reductions of 2.3, 1.7 and 1.2 orders were achieved for DTPA, EDTA and EDDS, respectively. However, during the first hour the inactivation curves for the three chelating agents were similar. For EDDS slight reduction of TC was

observed from 30 minutes until the end of the experiment. DTPA and EDTA followed the same trend than in MBR, achieving good results at the end of the experiment. The influence of chelate stability is pointed out again, according to Fig. 3. Figure 5 shows also that, depending on the effluent properties, the irradiation needed to achieve complete inactivation differ greatly. For instance, when DTPA was tested in MBR, total TC inactivation was achieved at 90 minutes, with an energy consumption of 0.47 $kJ \cdot L^{-1}$. However, in CAS, at 120 minutes of the treatment and an energy consumption of 0.63 $kJ \cdot L^{-1}$, the total inactivation had not been achieved. Turbidity and TOC of wastewater matrices can play an important role in these different behaviors.

It has been reported that the hydroxyl radicals formed in the photo-Fenton process can generate reactions affecting DNA, lipids and proteins, producing bacteria mortality [57, 58]. In addition, the bacterial inactivation can be explained by Fe(II) intracellular diffusion, where hydroxyl radicals can be generated during internal Fenton reactions [59, 60]. However, in photo-Fenton at neutral pH, using chelating agents, the presence of Fe(II) in solution is almost null, due to the fast formation of iron oxohydroxides and posterior precipitation. In addition, the diffusion of chelated iron (Ligand-Fe(II)) not likely to occur because of the high molecular weight. Concerning the action of iron oxohydroxides, controversy exists related to bacterial inactivation [61]. The formation of iron oxohydroxides due to the attack of hydroxyl radicals or the photo-degradation of the complex leave drive to a dissolution with high turbidity, which can scatter the light. Similar results were found by Samira and coworkers [62]. Apart from that, there is less dissolved iron in solution, which reduces the catalytic activity, generating less hydroxyl radicals. These facts can explain the differences between three iron complexes tested in this study. The iron complexes formed by EDDS and EDTA show the highest precipitation of iron and the lowest bacterial inactivation at the end of the treatment.

However, with DTPA-Fe(II) complex good results were found due to the less precipitation of iron.

Regarding *E.Coli,* the efficiency of three chelating agents was the same than TC: DTPA > EDTA > EDDS. At the end of the experiment, EDTA and DTPA achieved total *E.Coli* inactivation, being DTPA the best due to the total inactivation was reached at 90 minutes of the treatment.

An important parameter to take into account in wastewater reuse is the bacterial growth-on-the-plate. There are some pathogens, like *E. Coli*, that can manifest a "dormancy" mechanism during the treatment of WWs [63] and could turn into reactive under special conditions [64]. *E. Coli* and Total coliforms growth-on-the-plate was tested at the end of the experiment for EDTA, EDDS and DTPA and after 24, 48 and 72 hours from the accomplishment of the treatment. In figure 6, the bacterial growth-on-the-plates values are represented for TC (Fig. 6A) and *E. Coli* (Fig. 6B) in CAS and MBR matrices.
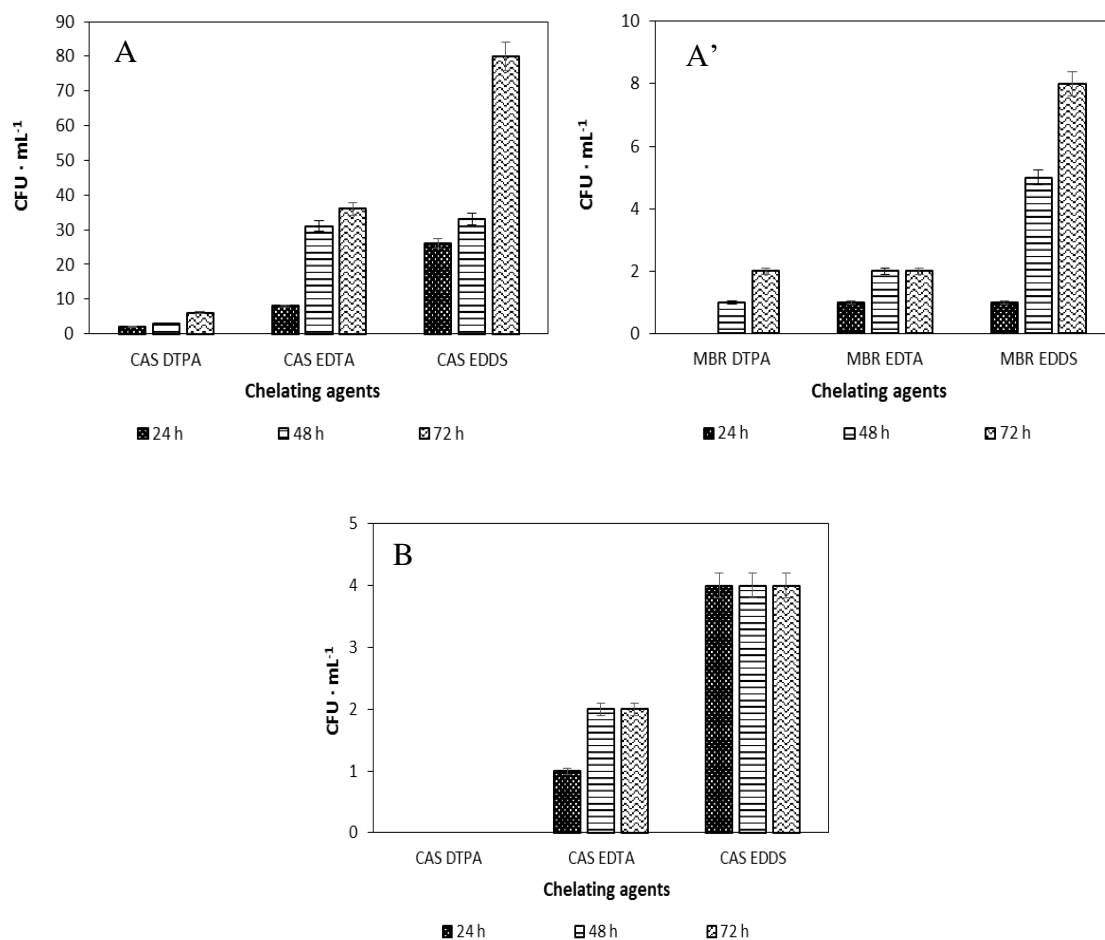
Figure 6. Bacterial growth-on-the-plates after 120 min of treatment for (A) Total Coliforms in CAS, (A') Total Coliforms in MBR and (B) *E. Coli* in CAS. $[PROP]_0 = 1.9 \ \mu M$; $[Fe(II)]_0 = 0.18 \ mM$; $[H_2O_2] = 4.41 \ mM$; $EDTA:Fe(II) = 1:1$; $DTPA:Fe(II) = 1:1$; $EDDS:Fe(II) = 2:1$.

The efficiency in bacterial growth-on-the-plates also depends on the quality of treated effluent. This was clearly seen in Fig. 6A where bacterial growth-on-the-plates of TC in CAS was higher than in MBR in all tested conditions. The introduction of DTPA as a chelating agent seems to be an enhancement for bacterial inactivation, as can be shown above. When DTPA was used in CAS, total coliforms were increased two times and three times at 48 and 72 hours, respectively. After 72 hours a value of 6 $CFU \cdot mL^{-1}$ was obtained, whilst in MBR after 72 hours 2 $CFU \cdot mL^{-1}$ were quantified. The differences

between the distinct WW matrices were also clearly observed when EDTA and EDDS were tested. The highest growth-on-the-plate was observed for EDDS in CAS, achieving 80 CFU·mL^{-1} after 72 h. Concluding, the growth-on-the-plate increases in the order: DTPA < EDTA < EDDS and, concerning WW matrix, CAS presents higher growth-on-the-plate than MBR.

Concerning *E. Coli* (Fig. 6B), no bacterial growth-on-the-plate was observed for DTPA. With EDTA, the bacterial growth-on-the-plate was observed from 24 to 48 hours. After this, no bacterial growth-on-the-plate was found. For EDDS, the bacterial growth-on-the-plate appears before 24 h and remains constant until 72 h. At 72 hours after the finalization of the photo-Fenton treatment the values for different chelating agents were 0, 2 and 4 CFU·mL^{-1}, for DTPA, EDTA and EDDS, respectively.

The differences observed for the chelating agents lie in the different chemical and biochemical properties of each ligand. EDDS is more biodegradable than EDTA or DTPA. Thus, the microorganisms in the effluent can degrade this molecule causing better conditions for growth-on-the-plate. As a consequence, the lowest CFU·mL^{-1} at the end of the experiment was obtained with DTPA. Thus, it is normal that the growth-on-the plate was lower.

3.4. Biodegradability and toxicity assessments

Depending on the final purpose of reused water, the requirements for water quality can be different. As explained above, agriculture consumption reaches to 60-70% of the total fresh water in the world. The minimum requirements for agricultural wastewater reuse can be found in the Proposal for a Regulation of the European Parliament and of the Council, Annex I [3]. *E.Coli* (CFU·100 mL^{-1}) and BOD$_5$ (mg O$_2$·L^{-1}) are two important parameters listed in the Regulation. Thus, in this study biodegradability assays and

disinfection (section 3.2) were performed in different experimental conditions where toxicity assessments (*Vibrio Fishery* and Phytotoxicity) were carried out.

For phytotoxicity tests, *L. sativa* (lettuce) seeds, acquired at a market, were used according to standardized protocols [32, 65]. The values were expressed in percentage of germination index (GI) according to equations 2-4 [32]. These tests were performed for three chelating agents in MBR and CAS (Figure 7). The control tests were carried out in deionized water.

$$\% \ seed \ germination = \frac{germination \ \% \ in \ the \ sample}{germination \ \% \ in \ the \ control} \ x \ 100 \qquad \textbf{(Eq. 2)}$$

$$\% \ root \ growth = \frac{mean \ root \ lenght \ in \ the \ sample}{mean \ root \ lenght \ in \ the \ control} \ x \ 100 \qquad \textbf{(Eq. 3)}$$

$$Germination \ index = \frac{\% \ seed \ germination \ x \ \% \ root \ growth}{100} \qquad \textbf{(Eq. 4)}$$
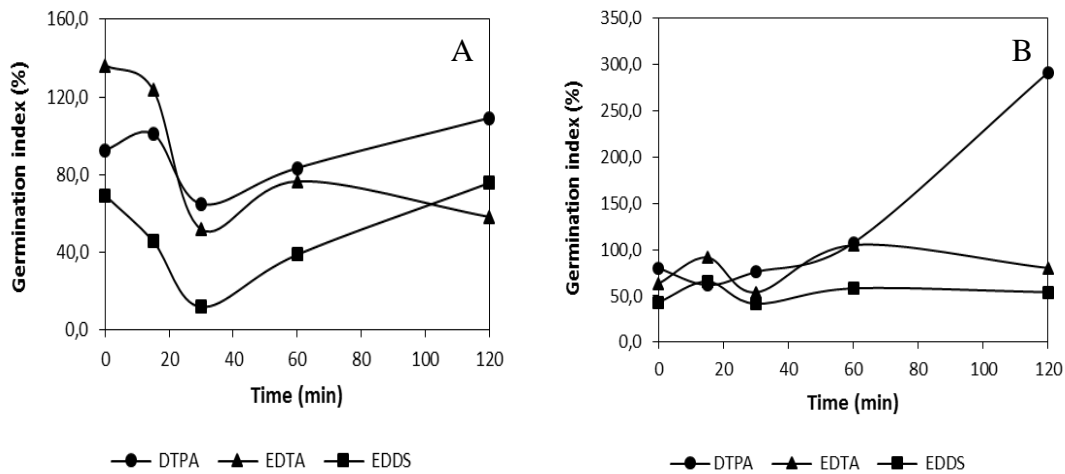
Figure 7. Percentage of germination index of *L. sativa* for different chelating agents (A) in MBR and (B) in CAS. [PROP]$_0$ = 1.9 μM; [Fe(II)]$_0$ = 0.18 mM; [H$_2$O$_2$] = 4.41 mM; EDTA:Fe(II) = 1:1; DTPA:Fe(II) = 1:1; EDDS:Fe(II) = 2:1.

Figure 7A shows that, at initial time, the effluent stimulated a root elongation only in EDTA with a germination index of 136%. For DTPA and EDDS the germination index at initial time was 93 and 69%, respectively, being DTPA similar to control test (which corresponds to 100% of germination index). Zucconi and co-workers explained that germination index above 80-85% indicate the disappearance of phytotoxicity and values above 50-60% of GI do not cause significant injury to the plant growth. However, GI lower than 20% indicates the inhibition of seed germination and root elongation. Values between 20 and 50% of GI indicates presence of phytotoxicity [66, 67]. At 30 minutes of the treatment, the germination indexes were the lowest in the three chelating agents (64.9, 51.9 and 11.9% for DTPA, EDTA and EDDS, respectively) indicating high phytotoxicity in EDDS. At the end of the treatment (120 min) for MBR the GI values of DTPA revealed stimulation of root elongation (GI = 109.3%). However, for EDTA and EDDS values of 58.2 and 75.8% of GI were achieved. Although these values were higher than these ones at 30 minutes, total disappearance of phytotoxicity were not observed. These results are in accordance with other studies where the toxicity increases in the middle of the treatment and at the end of the photo-Fenton process the toxicity decreases [68]. The phytotoxicity increase, achieved at 30 minutes of the treatment, could be associated to the formation of by-products more toxic than initial compound. Then, these by-products could be removed decreasing the toxicity. In addition, when DTPA was used and more toxic substances were removed, a favourable effect was observed at the end of the treatment. Concerning CAS, the same trend than in MBR was observed for the three chelating agents during the experiment. However, the changes in the phytotoxicity were less marked in CAS than in MBR for EDTA and EDDS. When DTPA was used, the values of germination index were similar to EDTA and EDDS during the first 60 minutes. Nevertheless, at the end of the experiment with DTPA, root elongation achieved a value

of 291.4% of GI. The fact that the changes in germination index were higher in CAS than in MBR could be the presence of compounds that in low concentrations can act as a micronutrient leading to the stimulation of the root elongation. Real photos of measurements of *L.Sativa* can be found in supplementary material (Figure S3 and Figure S4). In addition, values of number of germination seeds and mean root length (mm) for each condition tested were also included in supplementary material (Table S4).

Acute toxicity was studied with Microtox bioassay *(Vibrio Fishery).* In these experiments, same treatment times than for phytotoxicity were selected in order to establish comparisons. The two organisms showed different sensibilities during the experiment. Thus, no response was observed during the experiment with MBR or CAS for the three chelating agents when *Vibrio Fishery* was tested. In this way, *Lactuca sativa* demonstrated that was more sensitive than *Vibrio Fishery* in the evaluation of the effluent ecotoxicity.

Finally, the biodegradability was also evaluated since it is a parameter included in the Proposal for minimum requirements for agricultural water reuse. Figure 8 shows the BOD_5 in MBR and CAS for the three chelating agents.
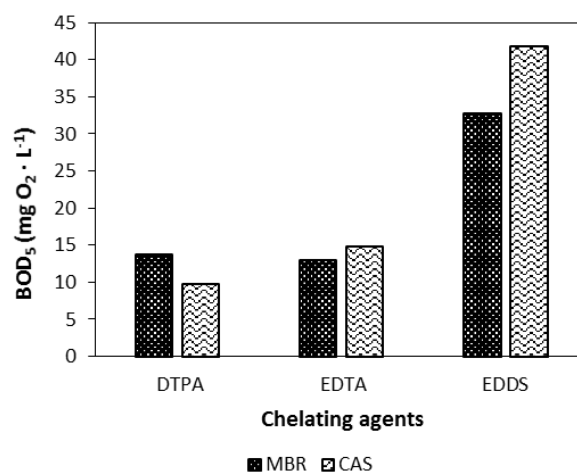
Figure 8. Biodegradability evaluation for EDTA, EDDS and DTPA in two WW (MBR and CAS). $[PROP]_0 = 1.9$ μM; $[Fe(II)]_0 = 0.18$ mM; $[H_2O_2] = 4.41$ mM; EDTA:Fe(II) = 1:1; DTPA:Fe(II) = 1:1; EDDS:Fe(II) = 2:1.

As it can be observed in Fig. 8, the biodegradability for EDDS was the highest in two WWs, being 32.8 and 41.8 mg $O_2 \cdot L^{-1}$ for MBR and CAS, respectively. EDTA and DTPA presented close values and always lower than 15 mg $O_2 \cdot L^{-1}$. The high biodegradability and the high L:Fe(II) molar ratio, when EDDS was employed, probably were two factors that influenced in these values.

The Proposal for agricultural water reuse [3] lists four reclaimed water qualities classes (A, B, C and D). Category A establishes a level ≤10 mg $O_2 \cdot L^{-1}$ of BOD_5. Categories from B to D establish a level ≤ 25 mg $O_2 \cdot L^{-1}$ of BOD_5. For *E. Coli*, the established levels are ≤ 10 CFU·100 mL^{-1}, ≤ 100 CFU·100 mL^{-1}, ≤ 1,000 CFU·100 mL^{-1} and ≤ 10,000 CFU·100 mL^{-1} for categories A, B, C and D, respectively (more information about the categories can be found in Table S5 of supplementary material). The values of *E.Coli* selected to discuss the categories, were at 72 hours after the end of the treatment. Therefore, when DTPA was used in CAS, at the end of the treatment the effluent satisfied the quality requirements of category A. In MBR matrix with DTPA, the effluent at the end of the treatment was included in category B. Finally, when EDTA was employed, the final effluent accomplished the requirements for the category C. In the case of EDDS, although the values for *E. Coli* satisfied the requirements for category C, the BOD_5 of the final effluent was higher than the level for water reuse for both wastewaters MBR and CAS. Thus, this effluent could not be reused for agriculture.

4. Conclusions

In this study, an organic fertilizer (DTPA) as a chelating agent of Fe^{2+} for neutral photo-Fenton was proven to be effective in simultaneous propranolol abatement and bacterial inactivation. MBR effluent (which is the cleanest matrix) showed higher propranolol degradation (94% of removal after 120 min) compared to other three wastewaters. Neutral photo-Fenton using DTPA was also effective for the disinfection of total coliforms and *E.Coli* in the different water matrices tested. Concerning wastewaters, the same trend was followed in bacterial inactivation than in propranolol removal.

Regarding the comparison of organic fertilizer with conventional chelating agents (EDTA and EDDS), EDTA showed better results in propranolol degradation (100% at 15 min) in MBR matrix but EDDS and DTPA show also good results (>90% at 120 min). In CAS matrix, the PROP removal was very similar for DTPA and EDTA. The observed differences are mainly related to the iron precipitation and the stability of the formed complex, being the complex DTPA:Fe(II) the more stable. In bacterial inactivation, DTPA showed the best results compared with the other chelating agents due to the stability of iron complexes. In addition, DTPA presented the lowest bacterial growth-on-the-plate for all conditions due to the internal damages that the complex produces.

The biodegradability for EDDS was the highest in two wastewaters and EDTA and DTPA presented close values. Regarding phytotoxicity, this increases in the middle of the treatment and at the end of the photo-Fenton process the toxicity decreases for three chelating agents, achieving DTPA the best germination index and the lower phytotoxicity.

Finally, when DTPA was used at the end of the treatment, the effluent satisfied the quality requirements for agricultural reuse.

References

[1] E. Ortega-Gómez, B. Esteban García, M.M. Ballesteros Martín, P. Fernández Ibáñez, J.A. Sánchez Pérez, Inactivation of natural enteric bacteria in real municipal wastewater by solar photo-Fenton at neutral pH, Water Research 63 (2014) 316-324.

[2] A. Rastogi, S.R. Al-Abed, D.D. Dionysiou, Effect of inorganic, synthetic and naturally occurring chelating agents on Fe(II) mediated advanced oxidation chlorophenols, Water Research 43 (2009) 684-694.

[3] European Commission, Proposal for a Regulation of the European Parliament and of the Council of 28 May 2018 establishing the minimum requirements for water reuse, Off. J. Eur. Communities. 337 (2018) 1-27.

[4] European Commission, Directive 2013/39/EU of the European Parliament and of the Council of 12 August 2013 amending Directives 2000/60/EC and 2008/105/EC as regards priority substances in the field of water policy, Off. J. Eur. Union. 226 (2013) 1-17.

[5] European Commission, Decision 2018/840/EU of 5 June establishing a watch list of substances for Union-wide monitoring in the field of water policy pursuant to Directive 2008/105/EC of the European Parliament and of the Council and repealing Decision 2015/495/EU, Off. J. Eur. Union. 141 (2018) 9-12.

[6] F.C. Moreira, R.A.R. Boaventura, E. Brillas, V.J. Vilar, Degradation of trimethoprim antibiotic by UVA photoelectron-Fenton process mediated by Fe(III)-carboxylate complexes, Applied Catalysis B: Enviromental 162 (2015) 34-44.

[7] R. Andreozzi, V. Caprio, A. Insola, R. Marotta, Advanced oxidation processes (AOP) for water purification and recovery, Catalysis Today 53 (1999) 51-59.

[8] B. Kasprzyk-Hordern, R.M. Dindsale, A.J. Guwy, The occurrence of pharmaceuticals personal care products, endocrine disruptors and illicit drugs in surface water in South Wales, UK, Water Research 42 (2008) 3498-3518.

[9] S. D. Kim, J. Cho, I.S. Kim, B.J. Vanderford, S.A. Synder, Occurrence and removal of pharmaceuticals and endocrine disruptors in South Korean surface drinking, and waste waters, Water Research 41 (2007) 1013-1021.

[10] P. Soriano-Molina, J.L. García Sánchez, O.M. Alfano, L.O. Conte, S. Malato, J.A. Sánchez Pérez, Mechanistic modeling of solar photo-Fenton process with Fe^{3+}-EDDS at neutral pH, Applied Catalysis B: Enviromental 233 (2018) 234-242.

[11] B. Quinn, F. Gagné, C. Blaise, An investigation into the acute and chronic toxicity of eleven pharmaceuticals (and their solvents) found in wastewater effluent on the cnidarian, Hydra attenuata, Science of Total Environment 389 (2008) 306-314.

[12] M.M. Schultz, E.T. Furlong, D.W. Kolpin, S.L. Werner, H.L. Schoenfuss, L.B. Barber, V.S. Blazer, D.O. Norris, A.M. Vajda, Antidepressant pharmaceuticals in two US effluent-impacted streams: occurrence and fate in water and sediment and selective uptake in fish neural tissue, Environmental Science Technology 44 (2010) 1918-1925.

[13] L. Clarizia, D. Russo, I. Di Somma, R. Marotta, R. Andreozzi, Homogeneous photo-Fenton processes at near neutral pH: A review, Applied Catalysis B: Environmental 209 (2017) 358-371.

[14] J. A. Lima Perini, A.L. Tonetti, C. Vidal, C.C. Montagner, R.F. Pupo Nogueira, Simultaneous degradation of ciprofloxacin, amoxicillin, sulfathiazole and sulfamethazine, and disinfection of hospital effluent after biological treatment via photo-Fenton process under ultraviolet germicidal irradiation, Applied Catalysis B: Environmental 224 (2018) 761-771.

[15] A. Fiorentino, R. Cucciniello, A. Di Cesare, D. Fontaneto, P. Prete, L. Rizzo, G. Corno, A. Proto, Disinfection of urban wastewater by a new photo-Fenton like process using Cu-iminodisucinic acid complex as catalyst at neutral pH, Water Research 146 (2018) 206-215.

[16] M. Català, N. Domínguez-Morueco, A. Migens, R. Molina. F. Martínez, Y. Valcárcel, N. Mastroianni, M. López de Alda, D. Barceló, Y. Segura, Elimination of drugs of abuse and their toxicity from natural Waters by photo-Fenton treatment, Science of Total Environment 520 (2015) 198-205.

[17] N. López-Vinent, A. Cruz-Alcalde, L.E. Romero, M.E. Chávez, P. Marco, J. Giménez, S. Esplugas, Synergies, radiation and kinetics in photo-Fenton process with UVA-LEDs, Journal of Hazardous Materials 380 (2019) 120882.

[18] S. Giannakis, M. Voumard, S. Rtimi, C. Pulgarin, Bacterial disinfection by the photo-Fenton process: Extracellular oxidation or intracellular photo-catalysis?, Applied Catalysis B: Environmental 227 (2018) 285-295.

[19] S. Miralles-Cuevas, D. Darowna, A. Wanag, S. Mozia, Malato S, I. Oller, Comparison of UV/H_2O_2, UV/$S_2O_8^{2-}$, solar/Fe(II)/H_2O_2 and solar/Fe(II)/$S_2O_8^{2-}$ at pilot plant scale for the elimination of micro-contaminants in natural water, Chemical Engineering Journal 310 (2017) 514–524.

[20] I. De la Obra, L. Ponce-Robles, S. Miralles-Cuevas, I. Oller, S. Malato, J.A. Sánchez Pérez, Microcontaminant removal in secondary effluents by solar photo-Fenton at circumneutral pH in raceway pond reactors, Catalysis Today 287 (2017) 10–14.

[21] W. Huang, M. Brigante, F. Wu, K. Hanna, G. Mailhot, Development of a new homogeneous photo-Fenton process using Fe(III)-EDDS complexes, Journal of Photochemistry and PhotobiolobyA: Chemistry 239 (2012) 17-23.

[22] Ministry of Agriculture, Fisheries and Food, Fertilizer products, (2019). https://www.mapa.gob.es/app/consultafertilizante/DetalleFertilizante.aspx?clave=1435# (accessed May 20, 2019).

[23] J. Maszkowska, S. Stolte, J. Kumirska, P. Łukaszewicz, K. Mioduszewska, A. Puckowski, M. Caban, M. Wagil, P. Stepnowski, A. Białk-Bielinska, Beta-blockers in the environment: Part I. Mobility and hydrolysis study, Science of the Total Environment 493 (2014) 1112–1121.

[24] C. Fernández, M. González-Doncel, J. Pro, G. Carbonell, J.V. Tarazona, Occurrence of pharmaceutically active compounds in surface waters of the Henares-Jarama-Tajo river system (Madrid, Spain) and a potential risk and characterization, Science of the Total Environment 408 (2010) 543-551.

[25] S.O. Ganiyu, N. Oturan, S. Raffy, G. Esposito, E. D. van Hullesbusch, M. Cretin, M.A. Oturan, Use of Sub-stoichiometric Titanium Oxide as a Ceramic Electrode in

Anodic Oxidation and Electro-Fenton Degradation of the Beta-blocker Propranolol: Degradation Kinetics and Mineralization Pathway, Electrochimica Acta 242 (2017) 344-354.

[26] R. P. Deo, Pharmaceuticals in the surface water of the USA: A review, Current Environmental Health Reports 1 (2014) 113-122.

[27] M. Gros, M. Petrovic, D. Barceló, Development of a multi-residue analytical methodology based on liquid chromatography-tandem mass spectrometry (LC-MS/MS) for screening and trace level determination of pharmaceuticals in surface and wastewaters, Talanta 70 (2006) 678-690.

[28] V. Gabet-Giraud, C. Miège, J.M. Choubert, S.M. Ruel, M. Coquery, Occurrence and removal of estrogens and beta blockers by various processes in wastewater treatment plants, Science of the Total Environment 408 (2010) 4257-4269.

[29] S. Terzic, I. Senta, M. Ahel, M. Gros. M. Petrovic, D. Barceló, J. Müller, T. Knepper, I. Martí, F. Ventura, P. Jovancic, D. Jabucar, Occurrence and fate of emerging wastewater contaminants in Western Balkan Region, Science of the Total Environment 399 (2009) 66-77.

[30] Y. Yang, J. Fu, H. Peng, L. Hou, M. Liu, J.L. Zhou, Occurrence and phase distribution of selected pharmaceuticals in Yangtze Estuary and its coastal zone, Journal of Hazardous Materials 190 (2011) 588-596.

[31] R.F. Pupo Nogueira, M.C. Oliveira, W.C. Paterlini, Simple and fast spectrophotometric determination of H_2O_2 in photo-Fenton reactions using metavanadate, Talanta 66 (2005) 86-89

[32] N.F.Y. Tam, S. Tiquia, Assessing toxicity of spent pig litter using a seed germination technique, Resources, Conservation and Recycling 11 (1994) 261-274.

[33] D. Schowanek, T.C.J. Feijtel, C.M. Perkins, F.A. Hartman, T.W. Federle, R.J. Larson, Biodegradation of [S,S], [R,R] and mixed stereoisomers of ethylene diamine disuccinic acid (EDDS), a transition metal chelator, Chemosphere 34 (11) (1997) 2375–2391.

[34] J.D. Englehardt, D.E. Meeroff, L. Echegoyen, Y. Deng, F.M. Raymo, T. Shibata, Oxidation of aqueous EDTA and associated organics and coprecipitation of inorganics by ambient iron-mediated aeration, Environmental Science and Technology 41 (2006) 270–276.

[35] S. Metsarinne, T. Tuhkanen, R. Aksela, Photodegradation of ethylenediaminetetraacetic acid (EDTA) and ethylenediamine disuccinic acid (EDDS) within natural UV radiation range, Chemosphere 45 (2001) 949–955.

[36] J. Li, 17β-Estradiol Degradation Photoinduced by Iron Complex, Clay and Iron Oxide Minerals: Effect of the Iron Complexing Agent Ethylenediamine-Ethylenediamine-N, N- Disuccinic Acid, University Blaise Pascal, Aubière, 2010, PhD Thesis.

[37] W. Huang, M. Brigante, F. Wu, C. Mousty, K. Hanna, G. Mailhot, Assessement of the Fe(III)-EDDS complex in Fenton-Like process: from the radical formation to the degradation of bisphenol A, Environmental Science and Technology 47 (2013) 1952-1959.

[38] B.H.J. Bielski, D.E. Cabelli, R.L. Arudi, A.B. Ross, Reactivity of HO_2/O_2^- radicals in aqueous solution, Journal of Physical and Chemical Reference Data 14 (1985) 1041–1100.

[39] A. De Luca, R.F. Dantas, S. Esplugas, Assessment of iron chelates efficiency for photo-Fenton at neutral pH, Water Research 61 (2014) 232-242.

[40] O. Abida, G. Mailhot, M. Litter, M. Bolte, Impact of iron-complex (Fe(III)-NTA) on photoinduced degradation of 4-chlorophenol in aqueous solution, Photochemical and Photobiology Science 5 (2006) 395–402.

[41] S.-P. Sun, X. Zeng, A.T. Lemley, Kinetics and mechanism of carbamazepine degradation by a modified Fenton-like reaction with ferric-nitrilotriacetate complexes, Journal of Hazardous Materials 252–253 (252) (2013) 155–165.

[42] L.I. Doumic, P.A. Soares, M.A. Ayude, M. Cassanello, R.A.R. Boaventura, V.J.P. Vilar, Enhancement of a solar photo-Fenton reaction by using ferrioxalate complexes for the treatment of a synthetic cotton-textile dyeing wastewater, Chemical Engineering Journal 277 (2015) 86–96.

[43] I.N. Dias, B.S. Souza, J.H.O.S. Pereira, F.C. Moreira, M. Dezotti, R.A.R. Boaventura, V.J.P. Vilar, Enhancement of the photo-Fenton reaction at near neutral pH through the use of ferrioxalate complexes: a case study on trimethoprim and sulfamethoxazole antibiotics removal from aqueous solutions, Chemical Engineering Journal 247 (2014) 302–313.

[44] N. Klamerth, S. Malato, M.I. Maldonado, A. Agüera, A.R. Fernandez-Alba, Modified photoFenton for degradation of emerging contaminants in municipal wastewater effluents, Catalysis Today 161 (2011) 241–246.

[45] X. Ou, X. Quan, S. Chen, F. Zhang, Y. Zhao, Photocatalytic reaction by Fe(III)-citrate complex and its effect on the photodegradation of atrazine in aqueous solution, Journal of Photochemical and Photobiology A 197 (2008) 382–388.

[46] M.R.A. Silva, A.G. Trovo, R.F.P. Nogueira, Degradation of the herbicide tebuthiuron using solar photo-Fenton process and ferric citrate complex at circumneutral pH, Journal of Photochemical and Photobiology A 191 (2007) 187–192.

[47] H. Katsumata, S. Kaneco, T. Suzuki, K. Ohta, Y. Yobiko, Photo-Fenton degradation of alachlor in the presence of citrate solution, Journal of Photochemical and Photobiology A 180 (2006) 38–45.

[48] P. Kocot, A. Karocki, Z. Stasicka, Photochemistry of the Fe(III)-EDTA complexes A mechanistic study, Journal of Photochemical and Photobiology A 179 (2006) 176–183.

[49] J.J. Pignatello, E. Oliveros, A. MacKay, Advanced oxidation processes for organic contaminant destruction based on the Fenton reaction and related chemistry. Critical Review of Environmental Science and Technology 36 (1) (2006) 1-84.

[50] J. Li, G. Mailhot, F. Wu, N. Deng, Photochemical efficiency of Fe(III)-EDDS complex: OH radical production and 17_-estradiol degradation, Journal of Photochemical and Photobiology A 212 (2010) 1–7.

[51] N. Klamerth, S. Malato, A. Agüera, A.R. Fernandez-Alba, G. Mailhot, Treatment of municipal wastewater treatment plant effluents with modified photo-Fenton as a tertiary treatment for the degradation of micro pollutants and disinfection, Environmental Science and Technology 46 (2012) 2885–2892

[52] S. Miralles-Cuevas, I. Oller, J.A.S. Perez, S. Malato, Removal of pharmaceuticals from MWTP effluent by nanofiltration and solar photo-Fenton using two different iron complexes at neutral pH, Water Research 64 (2014) 23–31.

[53] Dojindo Molecular Technologies, Inc, Table of Stability Constants, (2020). https://www.dojindo.com/images/Product%20Photo/Chelate_Table_of_Stability_Const ants.pdf (accessed January 15, 2019).

[54] N. López-Vinent, A. Cruz-Alcalde, C. Gutiérrez, P. Marco, J. Giménez, S. Esplugas, Micropollutant removal in WW by photo-Fenton (circumneutral and acid pH) with BLB and LED lamps, Chemical Engineering Journal 379 (2020) 122416.

[55] K. Davididou, E. Chatzisymeon, L. Pérez-Estrada, I. Oller, S. Malato, Photo-Fenton treatment of saccharin in a solar pilot compound parabolic collector: Use of olive mill wastewater as iron chelating agent, preliminary results, Journal of Hazardous Materials 372 (2019) 137-144.

[56] M.C. Collivignarelli, A. Abbà, I. Benigna, S. Sorlini, V. Torretta, Overview of the main disinfection processes for wastewater and drinking water treatment plants, Sustainability 10(1) (2018) 86

[57] D. Spuhler, A.J. Rengifo-Herrera, C. Pulgarin, The effect of Fe^2+, Fe^{3+}, H_2O_2 and the photo-Fenton reagent at near neutral pH on the solar disinfection (SODIS) at low temperatures of water containing Escherichia coli K12, Applied Catalysis: B Environmental 96 (2010) 126-141.

[58] I. García-Fernández, M. Polo-López, I. Oller, P. Fernández-Ibáñez, Bacteria and fungi inactivation using Fe^{3+}/sunlight, H_2O_2/sunlight and near neutral photo-Fenton: a comparative study, Applied Catalysis: B Environmental 121-122 (2012) 20-29.

[59] B. Halliwell, J. Gutterridge, Oxygen toxicity, oxygen radicals, transition metals and disease, Biochemical Journal 219 (1984) 1-14.

[60] M.I. Polo-López, I. Oller, P. Fernández-Ibáñez, Benefits of photo-Fenton at low concentrations for solar disinfection of distilled water. A case study: Phytophthora capsici, Catalysis Today 209 (2013) 181-187.

[61] J. Rodríguez-Chueca, M. Polo-López, R. Mosteo, M. Ormad, P. Fernández-Ibáñez, Disinfection of real and simulated urban wastewater effluents using a mild solar photo-Fenton, Applied Catalysis B: Environmental 150 (2014) 619-629.

[62] S. Nahim-Granados, I. Oller, S. Malato, J.A. Sánchez Pérez, M.I. Polo-López, Commercial fertilizer as effective iron chelate ($Fe3+$-EDDHA) for wastewater disinfection under natural sunlight for reusing in irrigation, Applied Catalysis B: Environmental 253 (2019) 286-292.

[63] A.R. Grupte, C.L.E. de Rezende, S.W. Joseph, Induction and resuscitation of viable but nonculturable Salmonella enterica serovar typhimurium DT104, Applied and Environmental Microbiology 69 (11) (2003) 6669-6675.

[64] J.D. Oliver, The viable but nonculturable state in bacteria, The journal of microbiology 43(S) (2005) 93-100.

[65] US EPA, Protocols for short term toxicity screening of hazardous waste sites. A. 8.7, Lettuce root elongation (*Latuca sativa*). EUA, Chicago (1989).

[66] F. Zucconi, A. Pera, M. Forte, Evaluating toxicity of immature compost, Biocycle (1981a) 54-57.

[67] F. Zucconi, M. Forte, A. Monaco, Biological evaluation of compost maturity, Biocycle (1981b) 27-29.

[68] A. M. Freitas, G. Rivas, M.C. Campos-Mañas, J.L. Casas López, A. Agüera, J.A. Sánchez Pérez, Ecotoxicity evaluation of a WWTP effluent treated by solar photo-Fenton at neutral pH in a raceway pond reactor, Environmental Science Pollution Research 24 (2017) 1093-1104.

Supplementary Information for

Organic fertilizer as a chelating agent in photo-Fenton at neutral pH with LEDs for agricultural wastewater reuse: micropollutant abatement and bacterial inactivation

N. López-Vinent, A. Cruz-Alcalde, Jacqueline A. Malvestiti, P. Marco, J. Giménez*, S. Esplugas

Department of Chemical Engineering and Analytical Chemistry, Faculty of Chemistry, Universitat de Barcelona, C/Martí i Franqués 1, 08028 Barcelona, Spain.
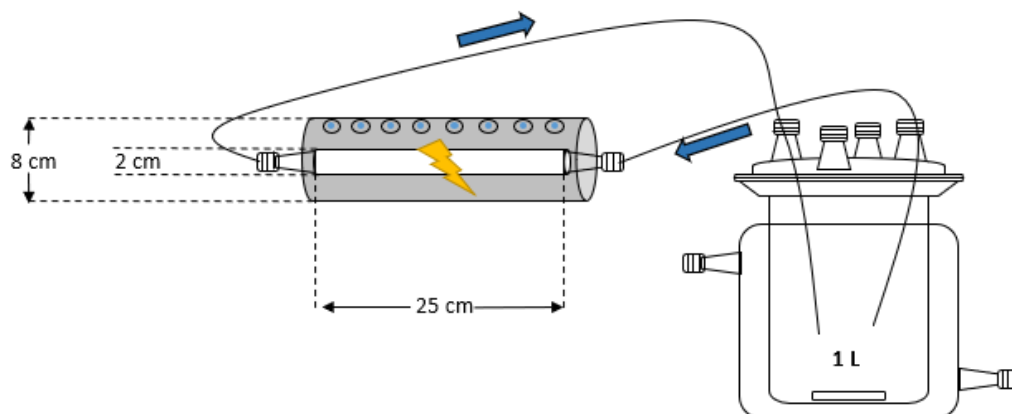
*Corresponding author:
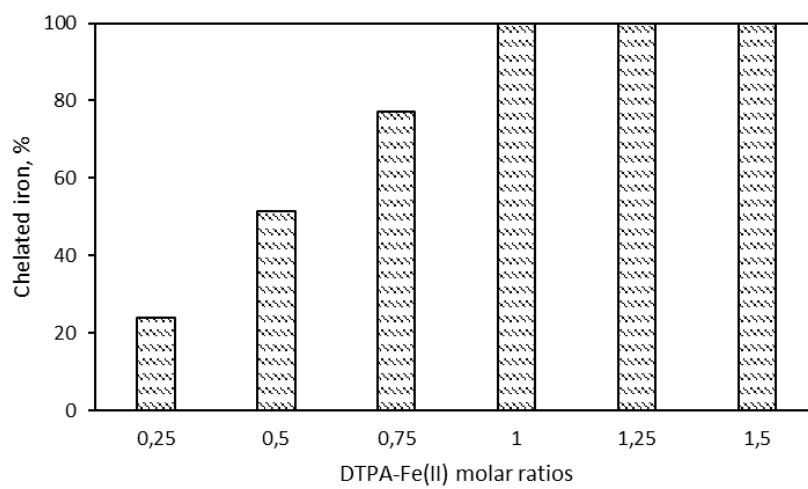Jaime Giménez Farreras, phone: +34 934 02 01 54, e-mail: j.gimenez.fa@ub.edu

Table of Contents

Figure S1. Experimental setup

Figure S2. Percentage of chelated iron for six DTPA-Fe(II) molar ratios tested.

Table S1. Conditions for the determination of the phytotoxicity with *Lactuca sativa* [1]

Parameters	Conditions
Temperature	22.0 ºC
Light	No
Test volume	4 mL per plate
Control	Distilled water
Number of seeds	10 seeds
Test duration	5 days
Test vessel	100 x 10 mm culture plate with 1 filter paper

Table S2. Degradation of propranolol by photo-Fenton at neutral pH with different Ligand-Fe(II) molar ratios. [PROP]= 0.19 mM; [H$_2$O$_2$]= 4.41 mM; [Fe(II)]= 0.18 mM.

DTPA:Fe(II) molar ratio	PROP removal (%) at 120 minutes
0.25:1	27.58
0.50:1	31.79
0.75:1	36.40
1:1	48.11
1.25:1	25.51
1.50:1	21.37

In that case, as a preliminary tests, the experiments, shown in Figure S2 and Table S2, were performed with 0.19 mM of target compound in order to see better the differences between different Ligand:Fe(II) molar ratios.

Table S3. Kinetic constants obtained for photo-Fenton at circumneutral pH. Values of R^2 of k_1 are not shown due to only two points were selected ($R^2= 1$).

| WW	Chelating agent	k_1 (min^{-1})	k_2 (min^{-1})	R^2 k_2	k_3 (min^{-1})	R^2 k_3
	EDTA	0.397	0.252	0.97	-	-
MBR	EDDS	0.438	0.085	0.97	0.009	0.84
	DTPA	0.324	0.038	0.97	0.020	0.97
	EDTA	0.339	0.020	0.98	0.007	0.94
CAS	EDDS	0.331	0.025	0.96	0.002	0.95
	DTPA	0.375	0.007	0.82	0.006	0.95

Table S3 shows the different kinetic constants for each chelating agent in MBR and CAS. These kinetics constants were performed in order to evidence the importance of the complex stability as explained above. The first order kinetic constants were calculated according to equation 1. Three kinetics were performed: k_1 is the kinetic constant at first 30 seconds of the treatment, k_2 is the kinetic constant from 30 seconds until 15 minutes (from this time the PROP degradation significantly slowed down in EDDS) and k_3 is the kinetic constant between 15 and 120 minutes.

Obviously, the fact of making three different fittings for each experiment comes out of what is a classical kinetic fitting. In this case, more than obtaining rigorous kinetic constants, it was intended to quantify the different behaviors observed throughout the same experiment. In this way, the influence on the MP degradation rate of the light, the type of chelating agent, the precipitation of the iron and the type of residual water can be explained in a pseudo-quantitative manner. Therefore, it has simply been tried to explain in a pseudo-quantitative way the shape of the graphs of figures 2 and 3 of the paper and the relationships among them.

References

[1] N.F.Y. Tam, S. Tiquia, Assessing toxicity of spent pig litter using a seed germination technique, Resources, Conservation and Recycling 11 (1994) 261-274.

[2] European Commission, Proposal for a Regulation of the European Parliament and of the Council of 28 May 2018 establishing the minimum requirements for water reuse, Off. J. Eur. Communities. 337 (2018) 1-27.
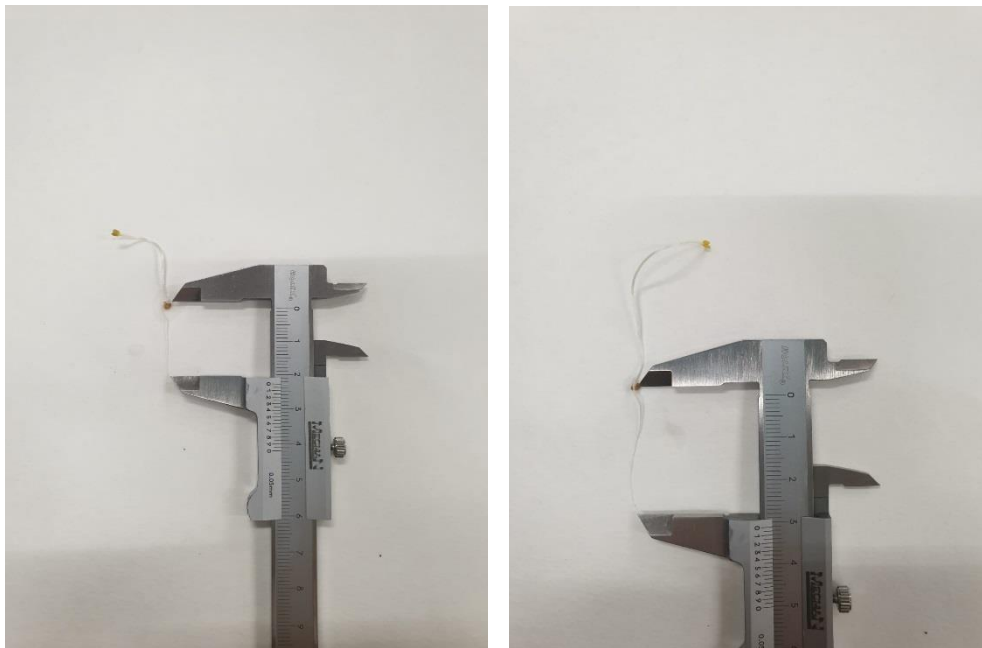
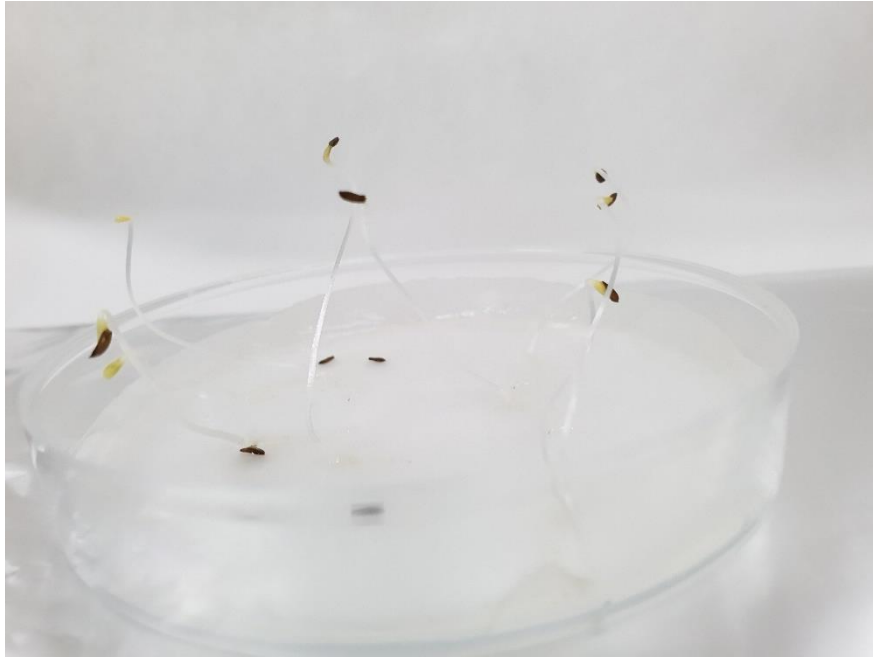**Figure S3. Measurement of root growth of *L. Sativa* to calculate the germination index**

Figure S4. Evaluation the number of _L. Sativa_ seeds germination

Table S4. Number of seed germination and mean root length (mm) of 10 seeds of _L. Sativa_

		Time (min)					Time (min)				
		0	**15**	**30**	**60**	**120**	**0**	**15**	**30**	**60**	**120**
		Number of seed germination (0/10)					**Mean root length (mm)**				
	DTPA	10	10	8	9	10	8.9	9.7	7.8	8.9	10.5
MBR	**EDTA**	10	9	6	8	8	13.1	13.2	8.3	9.2	7.0
	EDDS	7	6	3	6	8	9.5	7.3	3.8	6.2	9.1
	DTPA	8	6	9	10	10	9.6	9.9	8.1	10.3	28.0
CAS	**EDTA**	8	8	7	9	7	7.6	11.0	7.4	11.2	11.0
	EDDS	9	10	8	8	8	4.6	6.3	5.0	7.1	6.5
Control (mean)		8.5					11.3				

Table S5. Classes of reclaimed water quality and allowed agricultural use and irrigation method [2]

Minimum reclaimed water quality class	Crop category	Irrigation method
A	Food crops, including root crops consumed raw and food crops where the edible part is in direct contact with reclaimed water	All
B & C	Food crops consumed raw where the edible part is produced above ground and is not in direct contact with reclaimed water, processed food crops and non-food crops including crops to feed milk- or meat-producing animals	All
		Drip *
D	Industrial, energy, and seeded crops	All

(*) Drip irrigation (also called trickle irrigation) is a micro-irrigation system capable of delivering water drops or tiny streams to the plants and involves dripping water onto the soil or directly under its surface at very low rates (2-20 liters/hour) from a system of small diameter plastic pipes fitted with outlets called emitters or drippers.